BG Pulse Journal USA
ISSN:1947-2536 http://www.bgpulseusa.com/index.php/bg
BG PULSE JOURNAL

UDC 611.61:616-008.9

MORPHOLOGICAL FEATURES OF THE BLOOD VESSELS OF THE RENAL CORTEX IN EXPERIMENTAL METABOLIC SYNDROME

Sh. Q. Qosimova

Master's student, Department of Human Anatomy and Operative Surgery with Topographic Anatomy, Tashkent State Medical University, Tashkent, Uzbekistan

I. A. Tilyabov

PhD, Acting Associate Professor, Department of Human Anatomy and Operative Surgery with Topographic Anatomy, Tashkent State Medical University, Tashkent, Uzbekistan (scientific supervisor)

e-mail: shahnozaqosimova770@gmail.com , tel.: +998 91 194 28 07

Abstract

Background. Metabolic syndrome (MS) affects roughly one in four adults worldwide and is an independent risk factor for chronic kidney disease. The vascular bed of the renal cortex – interlobular arteries, afferent and efferent arterioles, glomerular and peritubular capillaries – is one of the earliest targets of metabolic injury, yet its structural remodelling in MS remains insufficiently characterised.

Aim. To study the morphological features of the blood vessels of the renal cortex in experimental metabolic syndrome, to identify the structural changes developing in the microcirculatory bed, and to evaluate their relationship with the state of the nephron.

Materials and methods. Metabolic syndrome was induced in male outbred white rats (n = 20) by a high-fat, high-fructose diet for 12 weeks; intact animals (n = 20) served as controls. Paraffin sections of the renal cortex were stained with haematoxylin and eosin and periodic acid–Schiff (PAS), examined immunohistochemically for TGF-β1 and subjected to morphometric analysis.

Results. In the experimental group, the renal cortex showed marked plethora and stasis in the glomerular and peritubular capillaries and venules, dilatation of the tubular lumina with flattening, vacuolisation and partial desquamation of the epithelium, interstitial oedema, perivascular cellular infiltration and expansion of the perivascular connective tissue. Immunohistochemistry revealed intense immunoreactivity in the periglomerular, perivascular and peritubular interstitium and in the basolateral compartment of the tubular epithelium (score 2.4 ± 0.2 vs 0.8 ± 0.1 in controls). The wall-to-lumen ratio of afferent arterioles increased from 0.36 ± 0.02 to 0.64 ± 0.03, peritubular capillary density decreased by 22.0%, the glomerular tuft area increased by 19.8% and the height of the proximal tubular epithelium decreased by 26.8% ($p < 0.01–0.001$).

Conclusion. Experimental metabolic syndrome is accompanied by complex remodelling of the cortical vascular bed of the kidney, in which microcirculatory disturbances and perivascular changes accompany and probably precede tubulointerstitial injury. These changes can be regarded as early morphological markers of metabolic nephropathy.

Keywords: metabolic syndrome, kidney, renal cortex, microcirculation, arterioles, peritubular capillaries, glomerulus, morphology, immunohistochemistry.

Introduction

Metabolic syndrome is a cluster of interrelated metabolic and haemodynamic disorders – abdominal obesity, hyperglycaemia and insulin resistance, arterial hypertension and atherogenic dyslipidaemia – that together markedly increase the risk of cardiovascular disease and type 2 diabetes mellitus [1]. According to current epidemiological estimates, MS is found in about 20–25% of the adult population of the world, and its prevalence continues to rise in parallel with the global epidemic of obesity and sedentary lifestyle [2].

The kidney is one of the principal target organs of MS. Large population-based studies have shown that the presence of MS and the number of its components are associated with an increased risk of chronic kidney disease and microalbuminuria [3], and a meta-analysis of prospective cohorts confirmed that MS is an independent predictor of incident chronic kidney disease [4]. In patients with established kidney disease, MS is associated with progression to end-stage renal disease [5]. Importantly, renal biopsy studies in non-diabetic individuals with MS have demonstrated arteriolar hyalinosis, glomerulomegaly, tubular atrophy and interstitial fibrosis even when kidney function was still within the normal range [6].

The mechanisms linking MS to renal injury are multifactorial. Insulin resistance and compensatory hyperinsulinaemia, activation of the renin–angiotensin–aldosterone and sympathetic nervous systems, oxidative stress, chronic low-grade inflammation and ectopic lipid accumulation ("fatty kidney") all converge on the renal microvasculature [7–9]. Afferent arteriolar vasodilatation combined with efferent vasoconstriction leads to glomerular hypertension and hyperfiltration, which in the long term cause glomerular enlargement, podocyte stress and focal segmental glomerulosclerosis – the morphological picture of obesity-related glomerulopathy [10, 11]. Lipotoxicity, in turn, damages the endothelium, mesangial cells and proximal tubular epithelium [9, 12].

The renal cortex receives about 90% of total renal blood flow and contains a unique vascular architecture: interlobular (cortical radiate) arteries give rise to afferent arterioles, which form the glomerular capillary tuft; blood then leaves through efferent arterioles and enters the peritubular capillary network that supplies the tubules. Because of this "portal" arrangement, any damage to the arterioles or glomerular capillaries is directly transmitted to the peritubular circulation. Injury and rarefaction of peritubular capillaries lead to chronic hypoxia of the tubulointerstitium, which is regarded as a final common pathway of progressive kidney disease [13, 14].

Despite the abundance of clinical and biochemical data, the structural mechanisms of renal damage in MS remain insufficiently studied. Most investigations have focused on the cardiovascular and endocrine systems, while information on the morphology of the renal microcirculatory bed – especially at the early, clinically silent stages of the disease – is limited and contradictory. Experimental models of diet-induced MS in rodents reproduce the key features of the human syndrome and allow the kidney to be examined at strictly defined time points [15–17]. Fructose-fed rats, for example, develop glomerular hypertension and afferent arteriolopathy [18, 19].

The aim of the present study was to investigate the morphological features of the blood vessels of the renal cortex in experimental metabolic syndrome, to identify the structural changes occurring in the microcirculatory bed, and to evaluate the relationship between these changes and the structural state of the nephron.

Materials and methods

Experimental animals and study design

The study was carried out on 40 male outbred white rats aged 3 months and weighing 180–200 g. The animals were kept in the vivarium of Tashkent State Medical University under standard conditions (temperature 22 ± 2 °C, 12-h light/dark cycle, free access to food and water). All procedures complied with the European Convention for the Protection of Vertebrate Animals Used for Experimental and Other Scientific Purposes (Strasbourg, 1986) and were approved by the Ethics Committee of Tashkent State Medical University. The study was reported in accordance with the ARRIVE guidelines [20].

The animals were randomly divided into two groups. The control group (n = 20) received standard laboratory chow and drinking water. In the experimental group (n = 20), metabolic syndrome was modelled by a high-fat diet (standard chow supplemented with 20% animal fat) combined with a 20% fructose solution as the only source of drinking fluid for 12 weeks, an approach widely used to reproduce obesity, insulin resistance, dyslipidaemia and hypertension in rodents [15–17].

Verification of the model

The development of MS was confirmed by dynamic measurement of body weight and abdominal circumference, fasting blood glucose and an oral glucose tolerance test, serum triglycerides, total cholesterol and high-density lipoprotein cholesterol, and systolic blood pressure measured by the non-invasive tail-cuff method. An animal was considered to have MS when at least three of these indicators differed significantly ($p < 0.05$) from control values.

Tissue sampling and histological processing

At the end of the experiment the animals were euthanised under ketamine–xylazine anaesthesia (80 and 10 mg/kg, intraperitoneally). Both kidneys were removed, weighed and cut along the frontal plane through the hilum. Tissue samples were fixed in 10% neutral buffered formalin for 24–48 h, dehydrated in ascending concentrations of ethanol, cleared in xylene and embedded in paraffin. Sections 4–5 µm thick were stained with haematoxylin and eosin (H&E) for general morphology and with the PAS reaction and Masson's trichrome for the evaluation of basement membranes, hyaline deposits and connective tissue.

Immunohistochemistry

Immunohistochemical staining was performed on deparaffinised sections after heat-induced antigen retrieval in citrate buffer (pH 6.0). Endogenous peroxidase activity was blocked with 3% hydrogen peroxide. The sections were incubated with a rabbit polyclonal primary antibody against transforming growth factor-β1 (TGF-β1; dilution 1:200, overnight at 4 °C), followed by a polymer-based horseradish peroxidase detection system and visualisation with 3,3′-diaminobenzidine (DAB); nuclei were counterstained with Mayer's haematoxylin. Negative controls were obtained by

omitting the primary antibody. The intensity of staining was assessed semi-quantitatively: 0 – no staining, 1 – weak, 2 – moderate, 3 – intense.

Morphometry and statistical analysis

Sections were examined with a binocular light microscope equipped with a digital camera. For each animal at least 10 randomly selected, non-overlapping fields of the cortex were analysed using ImageJ software (NIH, USA). The outer diameter and wall thickness of interlobular arteries, the lumen diameter, wall thickness and wall-to-lumen ratio of afferent arterioles, the glomerular tuft area, the width of Bowman's space, the diameter and density of peritubular capillaries, and the epithelial height and lumen diameter of the proximal tubules were measured. The data were processed with SPSS Statistics 26.0 (IBM, USA); results are expressed as the mean ± standard error (M ± m). Normality was checked with the Shapiro–Wilk test, and groups were compared with Student's t-test or the Mann–Whitney U-test as appropriate. Differences were considered significant at $p < 0.05$.

Results

General characteristics of the animals

By the end of the 12th week, all animals of the experimental group had developed the main components of MS. Compared with the control group, body weight was higher by 22.7% (312.4 ± 8.6 vs 254.7 ± 6.3 g), fasting blood glucose was 6.8 ± 0.3 vs 4.7 ± 0.2 mmol/L, serum triglycerides 2.14 ± 0.12 vs 0.96 ± 0.07 mmol/L, high-density lipoprotein cholesterol 0.82 ± 0.05 vs 1.21 ± 0.06 mmol/L, and systolic blood pressure 146.3 ± 3.2 vs 117.5 ± 2.4 mm Hg ($p < 0.001$ for all parameters).

Renal cortex of control animals

In control rats the renal cortex had a typical structure (Fig. 1A). Renal corpuscles were round, of uniform size and evenly distributed; the glomerular capillary loops were patent and filled with erythrocytes, and Bowman's space appeared as a narrow, regular crescent. The proximal convoluted tubules were lined by tall cuboidal epithelium with abundant eosinophilic granular cytoplasm and centrally located round nuclei; their lumina were narrow and slit-like. The distal tubules had a lower epithelium and wider, regular lumina. The interlobular arteries and arterioles had a thin intima, a well-defined media and no signs of hyalinosis. The peritubular capillaries were thin-walled, moderately filled with blood and closely adjacent to the tubular basement membranes; the interstitium was scant.

Renal cortex in experimental metabolic syndrome

In animals with MS pronounced changes were observed in all segments of the cortical vascular bed (Fig. 1B). The most characteristic finding was a disturbance of microcirculation: the peritubular capillaries and venules were dilated, overfilled with erythrocytes and in places showed signs of stasis and sludging. Elongated, blood-filled venules ran between the tubules, and in the region of the larger interlobular vessels the perivascular connective tissue was loosened, oedematous and expanded, with dilated, congested vasa vasorum and a focal cellular (predominantly mononuclear) infiltrate.

The tubular component of the cortex was significantly altered. The lumina of most proximal and distal tubules were markedly dilated and irregular in shape; the epithelium was flattened, the apical border was uneven, and many cells showed cytoplasmic vacuolisation and partial desquamation into the lumen. Eosinophilic flocculent material was present in a number of tubular lumina. In some zones the tubules were separated by widened oedematous interstitium, whereas in others areas of increased cellularity were seen. The renal corpuscles were heterogeneous: alongside corpuscles with plethoric capillary loops, there were glomeruli with a lobulated, partially retracted tuft and widened Bowman's space.

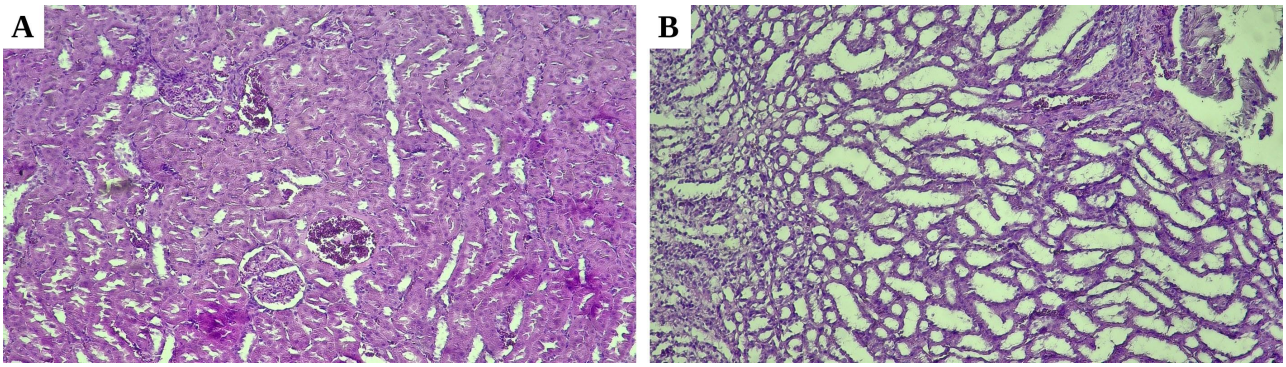


Figure 1. Renal cortex of the rat. A – control group: preserved architecture of renal corpuscles and convoluted tubules. B – experimental metabolic syndrome: dilatation of tubular lumina, flattening of the epithelium, congestion of interstitial vessels and expansion of the perivascular connective tissue. H&E, ×100.

Immunohistochemical findings

Immunohistochemical examination of the renal cortex in MS (Fig. 2) revealed a heterogeneous but generally increased expression of TGF-β1. At high magnification (Fig. 2A), a diffuse granular cytoplasmic reaction was observed in the tubular epithelium, with more intense linear staining along the basolateral surface of epithelial cells and in the walls of peritubular capillaries. The luminal content of dilated tubules was immunonegative.

At low magnification (Fig. 2B), the strongest immunoreactivity (score 3) was concentrated in the vascular–interstitial compartment: around the renal corpuscles, along the interlobular vessels and in the perivascular connective tissue surrounding large vessels, where it coincided with zones of cellular infiltration. The epithelium of the convoluted tubules adjacent to the vessels was also intensely stained, whereas tubules located farther from the vascular axes showed only weak to moderate reaction (score 1–2). The glomerular tuft itself showed weak staining, with moderate positivity of the parietal layer of Bowman's capsule. Thus, the distribution of immunoreactivity followed a clear perivascular gradient.

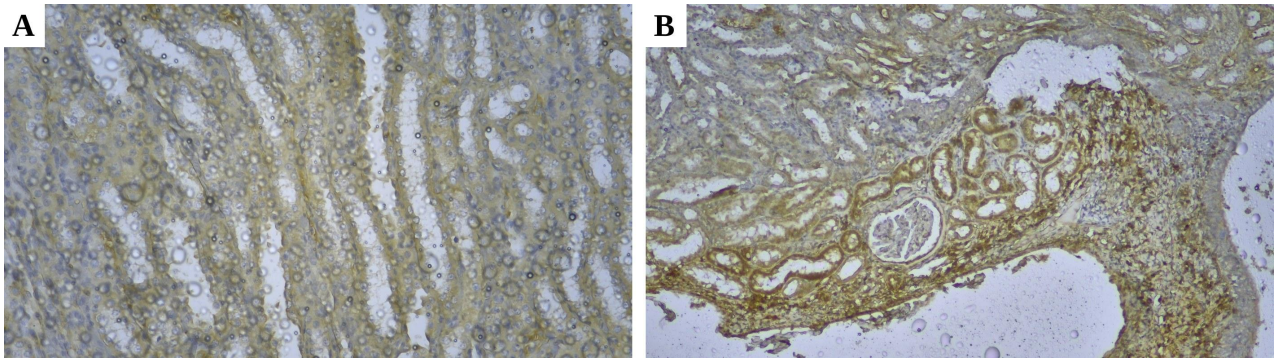


Figure 2. Renal cortex of the rat in experimental metabolic syndrome. A – diffuse cytoplasmic and basolateral immunoreactivity of the tubular epithelium, ×400. B – intense immunoreactivity in the periglomerular, perivascular and peritubular interstitium, ×100. Immunohistochemistry, DAB, counterstained with haematoxylin.

Morphometric data

Quantitative morphometric parameters of the vessels, renal corpuscles and tubules of the renal cortex in the control and experimental groups are summarised in Table 1. In MS the wall thickness of the interlobular arteries increased by 43.0% and that of the afferent arterioles by 45.1%, while the lumen of the afferent arterioles narrowed by 19.0%; as a result, the wall-to-lumen ratio of the afferent arterioles increased 1.8-fold. The glomerular tuft area increased by 19.8% and the width of Bowman's space by 45.2%. The peritubular capillaries were dilated (diameter +34.2%), but their density decreased by 22.0%, indicating early capillary rarefaction. The height of the proximal tubular epithelium decreased by 26.8%, whereas the tubular lumen widened by 70.8%.

Table 1

Morphometric parameters of the renal cortex in control rats and rats with experimental metabolic syndrome (M ± m)

Parameter	Control (n = 20)	MS (n = 20)	p
Interlobular artery: outer diameter, μm	62.4 ± 2.1	71.8 ± 2.6	< 0.01
Interlobular artery: wall thickness, μm	8.6 ± 0.4	12.3 ± 0.5	< 0.001
Afferent arteriole: lumen diameter, μm	14.2 ± 0.6	11.5 ± 0.5	< 0.01
Afferent arteriole: wall thickness, μm	5.1 ± 0.2	7.4 ± 0.3	< 0.001
Afferent arteriole: wall-to-lumen ratio	0.36 ± 0.02	0.64 ± 0.03	< 0.001
Glomerular tuft area, μm²	8450 ± 210	10120 ± 280	< 0.001
Width of Bowman's space, μm	4.2 ± 0.3	6.1 ± 0.4	< 0.01
Peritubular capillary diameter, μm	7.3 ± 0.3	9.8 ± 0.4	< 0.001
Peritubular capillary density, per field (×400)	24.6 ± 1.1	19.2 ± 0.9	< 0.01

Proximal tubule: epithelial height, μm	13.8 ± 0.4	10.1 ± 0.5	< 0.001
Proximal tubule: lumen diameter, μm	9.6 ± 0.5	16.4 ± 0.8	< 0.001
Immunohistochemical score, points (0–3)	0.8 ± 0.1	2.4 ± 0.2	< 0.001

Discussion

The present study demonstrates that experimental metabolic syndrome is accompanied by complex structural remodelling of the vascular bed of the renal cortex, involving the arteries and arterioles, the glomerular and peritubular capillaries and the surrounding interstitium. These findings are consistent with the concept that the renal microvasculature is one of the earliest and most sensitive targets of metabolic injury [7, 13].

The leading feature in our material was a disturbance of microcirculation in the form of plethora, dilatation and stasis in the peritubular capillaries and venules. In MS, hyperinsulinaemia and insulin resistance impair the phosphatidylinositol-3-kinase–endothelial nitric oxide synthase pathway, reduce nitric oxide bioavailability and shift the endothelium towards a vasoconstrictive, pro-inflammatory and pro-thrombotic phenotype [7, 8]. Combined with activation of the renin–angiotensin system, this leads to dilatation of the afferent and constriction of the efferent arterioles, glomerular hypertension and hyperfiltration [8, 11]. Experimental studies in fructose-fed rats have shown that these haemodynamic changes are accompanied by thickening of the afferent arteriolar wall and an increased wall-to-lumen ratio [18, 19], which corresponds to the arteriolar hyalinosis described in renal biopsies of patients with MS [6]. In our study, the 1.8-fold increase in the wall-to-lumen ratio of the afferent arterioles indicates that functional vasodilatation at the early stage is gradually replaced by structural remodelling of the arteriolar wall with narrowing of the lumen.

Because the peritubular capillaries originate from the efferent arterioles, glomerular haemodynamic disturbances are directly transmitted to the tubulointerstitial compartment. Congestion and slowing of blood flow in the peritubular network impair oxygen and substrate delivery to the metabolically highly active proximal tubular epithelium. The dilatation of tubular lumina, flattening, vacuolisation and desquamation of the epithelium observed in our study can therefore be regarded as a manifestation of combined hypoxic, haemodynamic (hyperfiltration-related) and lipotoxic injury [9, 12].

The heterogeneity of the renal corpuscles – coexistence of plethoric glomeruli with glomeruli showing tuft retraction and widened Bowman's space – reflects different stages of glomerular damage. Glomerular hyperperfusion and hypertrophy are characteristic of obesity-related glomerulopathy [10], whereas tuft retraction may indicate ischaemic injury of glomeruli supplied by structurally altered arterioles. Similar features have been described in renal biopsies of individuals with MS [6] and, at a later stage, in diabetic nephropathy [22].

The immunohistochemical findings are of particular interest. The maximum immunoreactivity was found in the periglomerular and perivascular interstitium, i.e. in the immediate vicinity of the altered vessels, and decreased with distance from the vascular axes. Together with perivascular oedema and cellular infiltration, this gradient indicates that the vessels act as the initial focus from which inflammatory and profibrotic changes spread into the tubulointerstitium. According to current concepts, endothelial damage and rarefaction of peritubular capillaries create a vicious circle of hypoxia, inflammation and fibrosis that underlies

the progression of chronic kidney disease [13, 14]. TGF-β1 is regarded as the key mediator of this process: it stimulates the transformation of fibroblasts and pericytes into myofibroblasts, the synthesis of extracellular matrix and the loss of peritubular capillaries [21]. The threefold increase in TGF-β1 expression and the 22% reduction in peritubular capillary density found in our study therefore reflect the onset of profibrotic remodelling. The detection of these changes in the experimental model, in the absence of advanced sclerosis, suggests that vascular remodelling is an early event in the pathogenesis of metabolic nephropathy and may precede a clinically manifest decline in renal function.

Some limitations of the study should be noted. The kidneys were examined at a single time point, and only light microscopy and immunohistochemistry were used; electron microscopic assessment of the glomerular basement membrane, endothelial fenestrae and podocytes, as well as a comparison of morphological parameters with functional indicators (serum creatinine, albuminuria), will be the subject of further research.

Conclusions

1. Experimental metabolic syndrome causes complex remodelling of the blood vessels of the renal cortex, manifested by plethora, dilatation and stasis in the peritubular capillaries and venules, perivascular oedema, cellular infiltration and expansion of the perivascular connective tissue, as well as by thickening of the walls of interlobular arteries (+43.0%) and afferent arterioles (+45.1%) with a 1.8-fold increase in the wall-to-lumen ratio.

2. Vascular changes are accompanied by tubular injury – dilatation of tubular lumina, flattening, vacuolisation and desquamation of the epithelium – and by heterogeneous changes of the renal corpuscles, ranging from glomerular plethora to tuft retraction with widening of Bowman's space.

3. The expression of TGF-β1 increases threefold, and the most intense reaction is localised in the periglomerular and perivascular interstitium and decreases with distance from the vessels, indicating that the microvascular bed is the initial site of injury in metabolic nephropathy.

4. The identified morphological changes of the cortical vascular bed can serve as early structural markers of renal damage in metabolic syndrome and as a morphological basis for its early diagnosis and prevention.

Practical significance

The results of the study provide a morphological basis for the early detection of microcirculatory changes in the kidney and for improving the pathomorphological diagnosis of the initial stages of metabolic syndrome. The data can be used in teaching and research in morphology, nephrology and endocrinology, and in developing strategies to prevent the renal complications of metabolic syndrome.

References

1. Alberti KGMM, Eckel RH, Grundy SM, Zimmet PZ, Cleeman JI, Donato KA, et al. Harmonizing the metabolic syndrome: a joint interim statement of the IDF Task Force on Epidemiology and Prevention; NHLBI; AHA; WHF; IAS; and IASO. Circulation. 2009;120(16):1640–1645.

2. Saklayen MG. The global epidemic of the metabolic syndrome. Curr Hypertens Rep. 2018;20(2):12.

3. Chen J, Muntner P, Hamm LL, Jones DW, Batuman V, Fonseca V, et al. The metabolic syndrome and chronic kidney disease in U.S. adults. Ann Intern Med. 2004;140(3):167–174.

4. Thomas G, Sehgal AR, Kashyap SR, Srinivas TR, Kirwan JP, Navaneethan SD. Metabolic syndrome and kidney disease: a systematic review and meta-analysis. Clin J Am Soc Nephrol. 2011;6(10):2364–2373.

5. Navaneethan SD, Schold JD, Kirwan JP, Arrigain S, Jolly SE, Poggio ED, et al. Metabolic syndrome, ESRD, and death in CKD. Clin J Am Soc Nephrol. 2013;8(6):945–952.

6. Alexander MP, Patel TV, Farag YMK, Florez A, Rennke HG, Singh AK. Kidney pathological changes in metabolic syndrome: a cross-sectional study. Am J Kidney Dis. 2009;53(5):751–759.

7. Wahba IM, Mak RH. Obesity and obesity-initiated metabolic syndrome: mechanistic links to chronic kidney disease. Clin J Am Soc Nephrol. 2007;2(3):550–562.

8. Hall JE, do Carmo JM, da Silva AA, Wang Z, Hall ME. Obesity, kidney dysfunction and hypertension: mechanistic links. Nat Rev Nephrol. 2019;15(6):367–385.

9. de Vries APJ, Ruggenenti P, Ruan XZ, Praga M, Cruzado JM, Bajema IM, et al. Fatty kidney: emerging role of ectopic lipid in obesity-related renal disease. Lancet Diabetes Endocrinol. 2014;2(5):417–426.

10. Kambham N, Markowitz GS, Valeri AM, Lin J, D'Agati VD. Obesity-related glomerulopathy: an emerging epidemic. Kidney Int. 2001;59(4):1498–1509.

11. Helal I, Fick-Brosnahan GM, Reed-Gitomer B, Schrier RW. Glomerular hyperfiltration: definitions, mechanisms and clinical implications. Nat Rev Nephrol. 2012;8(5):293–300.

12. Bobulescu IA. Renal lipid metabolism and lipotoxicity. Curr Opin Nephrol Hypertens. 2010;19(4):393–402.

13. Kang DH, Kanellis J, Hugo C, Truong L, Anderson S, Kerjaschki D, et al. Role of the microvascular endothelium in progressive renal disease. J Am Soc Nephrol. 2002;13(3):806–816.

14. Chade AR. Renal vascular structure and rarefaction. Compr Physiol. 2013;3(2):817–831.

15. Panchal SK, Brown L. Rodent models for metabolic syndrome research. J Biomed Biotechnol. 2011;2011:351982.

16. Wong SK, Chin KY, Suhaimi FH, Fairus A, Ima-Nirwana S. Animal models of metabolic syndrome: a review. Nutr Metab (Lond). 2016;13:65.

17. Lerman LO, Kurtz TW, Touyz RM, Ellison DH, Chade AR, Crowley SD, et al. Animal models of hypertension: a scientific statement from the American Heart Association. Hypertension. 2019;73(6):e87–e120.

18. Nakagawa T, Hu H, Zharikov S, Tuttle KR, Short RA, Glushakova O, et al. A causal role for uric acid in fructose-induced metabolic syndrome. Am J Physiol Renal Physiol. 2006;290(3):F625–F631.

19. Sánchez-Lozada LG, Tapia E, Jiménez A, Bautista P, Cristóbal M, Nepomuceno T, et al. Fructose-induced metabolic syndrome is associated with glomerular hypertension and renal microvascular damage in rats. Am J Physiol Renal Physiol. 2007;292(1):F423–F429.

20. Kilkenny C, Browne WJ, Cuthill IC, Emerson M, Altman DG. Improving bioscience research reporting: the ARRIVE guidelines for reporting animal research. PLoS Biol. 2010;8(6):e1000412.

21. Meng XM, Nikolic-Paterson DJ, Lan HY. TGF-β: the master regulator of fibrosis. Nat Rev Nephrol. 2016;12(6):325–338.

22. Tervaert TWC, Mooyaart AL, Amann K, Cohen AH, Cook HT, Drachenberg CB, et al. Pathologic classification of diabetic nephropathy. J Am Soc Nephrol. 2010;21(4):556–563.